nature medicine

Common noncoding *UMOD* gene variants induce salt-sensitive hypertension and kidney damage by increasing uromodulin expression

Matteo Trudu[1], Sylvie Janas[2,3], Chiara Lanzani[4], Huguette Debaix[2,3], Céline Schaeffer[1], Masami Ikehata[5,6], Lorena Citterio[4], Sylvie Demaretz[7], Francesco Trevisani[8], Giuseppe Ristagno[9], Bob Glaudemans[2], Kamel Laghmani[7], Giacomo Dell'Antonio[10], the Swiss Kidney Project on Genes in Hypertension (SKIPOGH) team[11], Johannes Loffing[12], Maria P Rastaldi[5,6], Paolo Manunta[8], Olivier Devuyst[2,3,13] & Luca Rampoldi[1,13]

Hypertension and chronic kidney disease (CKD) are complex traits representing major global health problems[1,2]. Multiple genome-wide association studies have identified common variants in the promoter of the *UMOD* gene[3–9], which encodes uromodulin, the major protein secreted in normal urine, that cause independent susceptibility to CKD and hypertension. Despite compelling genetic evidence for the association between *UMOD* risk variants and disease susceptibility in the general population, the underlying biological mechanism is not understood. Here, we demonstrate that *UMOD* risk variants increased *UMOD* expression *in vitro* and *in vivo*. Uromodulin overexpression in transgenic mice led to salt-sensitive hypertension and to the presence of age-dependent renal lesions similar to those observed in elderly individuals homozygous for *UMOD* promoter risk variants. The link between uromodulin and hypertension is due to activation of the renal sodium cotransporter NKCC2. We demonstrated the relevance of this mechanism in humans by showing that pharmacological inhibition of NKCC2 was more effective in lowering blood pressure in hypertensive patients who are homozygous for *UMOD* promoter risk variants than in other hypertensive patients. Our findings link genetic susceptibility to hypertension and CKD to the level of uromodulin expression and uromodulin's effect on salt reabsorption in the kidney. These findings point to uromodulin as a therapeutic target for lowering blood pressure and preserving renal function.

Current understanding of the complex genetic architecture of hypertension and CKD stems from the identification of mutations causing rare inherited disorders[10,11] and of several susceptibility loci through population-based association studies[12–14]. However, deciphering the biological mechanisms underlying these genetic associations has proven to be a major challenge.

Recent genome-wide association studies (GWAS) in more than 200,000 individuals of European ancestry have identified susceptibility variants for renal function, CKD and hypertension in the *UMOD* gene encoding uromodulin[3–9]. Uromodulin (or Tamm-Horsfall protein) is the most abundant urinary protein and is specifically produced and secreted by the epithelial cells lining the thick ascending limb (TAL) of the loop of Henle in the kidney[15]. Studies in *Umod* knockout mice revealed that uromodulin may protect against urinary tract infection[16] and kidney stones[17] and modulate electrolyte tubular transport[18]. Recent evidence suggests that uromodulin regulates the activity of the sodium-potassium-chloride transporter (NKCC2) and the renal outer medullary potassium channel (ROMK), the two main ion transporters involved in NaCl reabsorption by the TAL segment[19,20]. Mutations in *UMOD* have been associated with rare dominantly inherited disorders causing kidney damage and CKD[21]. The observation that susceptibility variants in the *UMOD* gene have a high frequency (about 0.8) in the general population and confer about 20% increased risk for CKD and 15% for hypertension emphasizes the pressing need to understand the nature of their associated risk and how they affect uromodulin function[22].

Given the localization of the most significant (lead) single nucleotide polymorphisms (SNPs) identified by GWAS in a linkage disequilibrium block that includes the *UMOD* gene promoter (**Fig. 1a**), we hypothesized that these variants could be associated with an effect on gene expression. We tested this hypothesis *in vivo* by measuring *UMOD* transcript levels in nephrectomy samples from individuals homozygous for either the risk or protective alleles at lead variants

[1]Dulbecco Telethon Institute, Division of Genetics and Cell Biology, San Raffaele Scientific Institute, Milan, Italy. [2]Institute of Physiology, Zurich Center for Integrative Human Physiology, University of Zurich, Zurich, Switzerland. [3]Division of Nephrology, Université catholique de Louvain, Medical School, Brussels, Belgium. [4]Division of Nephrology and Dialysis, San Raffaele Scientific Institute, Milan, Italy. [5]Renal Research Laboratory, Fondazione Istituto di Ricovero e Cura a Carattere Scientifico Ca' Granda, Ospedale Maggiore Policlinico, Milan, Italy. [6]Fondazione D'Amico per la Ricerca sulle Malattie Renali, Milan, Italy. [7]INSERM UMRS 872, Paris, France. [8]School of Nephrology, University Vita-Salute San Raffaele, Milan, Italy. [9]Department of Cardiovascular Research, Istituto di Ricerce Farmacologiche Mario Negri, Milan, Italy. [10]Department of Pathology, San Raffaele Scientific Institute, Milan, Italy. [11]Full list of members and affiliations appears at the end of the paper. [12]Institute of Anatomy, Zurich Center for Integrative Human Physiology, University of Zurich, Zurich, Switzerland. [13]These authors contributed equally to this work. Correspondence should be addressed to L.R. (rampoldi.luca@hsr.it) or O.D. (olivier.devuyst@uzh.ch).

Received 14 June; accepted 19 September; published online 3 November 2013; doi:10.1038/nm.3384

© 2013 Nature America, Inc. All rights reserved.
source: https://doi.org/10.7892/boris.48779 | downloaded: 13.3.2017

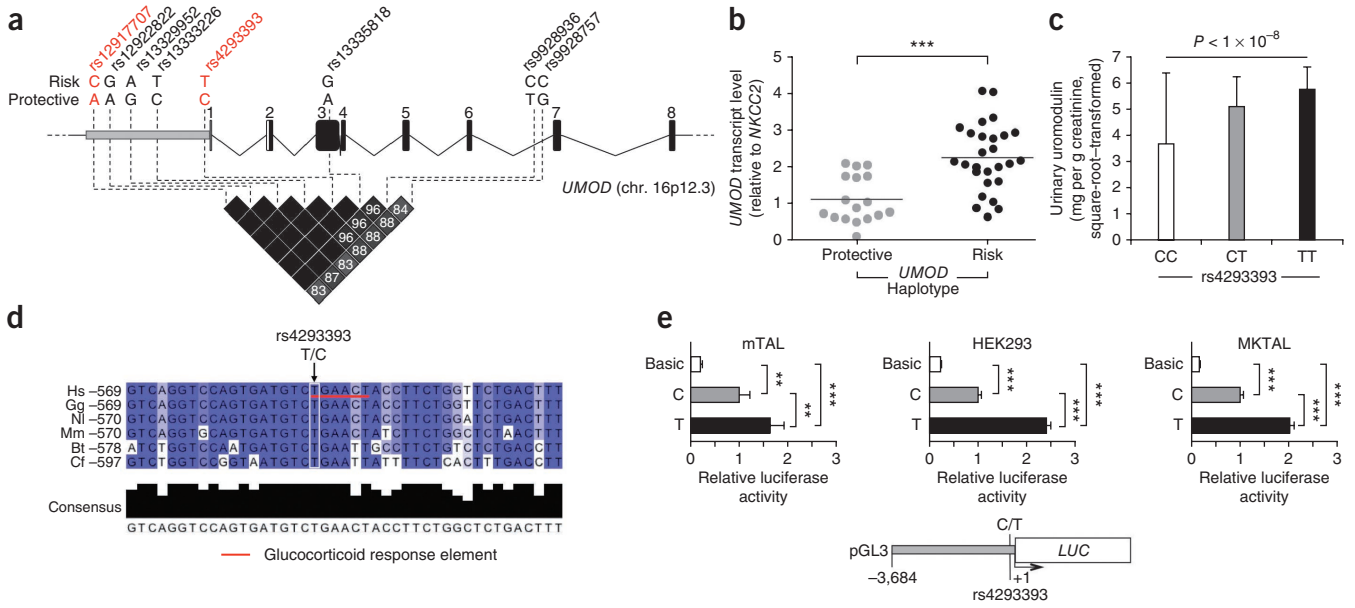

Figure 1 Effects of *UMOD* SNP variants on uromodulin expression. (**a**) Schematic representation of human *UMOD* gene structure. The positions of lead SNPs in the *UMOD* promoter associated with hypertension and CKD are shown. All variants are within the same linkage disequilibrium block, as shown by the linkage disequilibrium plot (r^2 values, data from HapMap CEU, release #28). Genotyped SNPs are shown in red. (**b**) *UMOD* expression levels (quantitative RT-PCR (qRT-PCR)) in nephrectomy samples of individuals homozygous for either protective ($n = 17$) or risk ($n = 27$) alleles for *UMOD* promoter variants rs12917707 and rs4293393. All samples were genotyped for both variants. We normalized *UMOD* expression to *NKCC2* to account for differing TAL content in the samples. Each dot represents an individual, and the distribution and mean values of expression levels are shown. ***$P < 0.001$ (Mann-Whitney test). (**c**) Urinary uromodulin concentrations in individuals of the SKIPOGH cohort by genotype at rs4293393 ($n = 18$ CC, $n = 214$ CT and $n = 532$ TT). Data are expressed as means ± s.e.m. The *P* value reflects significant association of rs4293393 genotype with square-root–transformed daytime urinary uromodulin-to-creatinine ratio in a mixed linear model. C, protective allele; T, risk allele. (**d**) Partial alignment of human (Hs), gorilla (Gg), gibbon (Nl), macaque (Mm), cow (Bt) and dog (Cf) *UMOD* promoter sequences. The intensity of the blue color shading corresponds to nucleotide conservation (the darker the color, the higher the degree of nucleotide conservation). The rs4293393 SNP is predicted to lie within a glucocorticoid response element; the protective (C) allele would disrupt this predicted binding site. T, risk allele. (**e**) Quantitative analysis of the relative effects of the protective (C) and risk (T) alleles of SNP rs4293393 on the transcriptional activity of *UMOD* promoter as assessed by a luciferase reporter assay in three types of kidney cells: mTAL, (highly differentiated mouse primary TAL cells retaining uromodulin expression), immortalized MKTAL (mouse kidney TAL) and HEK293 (human embryonic kidney) cells. The data are from four independent experiments. The schematic shows the luciferase reporter constructs used, in which a 3.7-kb *UMOD* promoter fragment containing either the C or T allele was cloned upstream of the firefly luciferase (*LUC*) gene in the pGL3-Basic reporter vector (Basic corresponds to the promoterless vector). Data are expressed as means ± s.e.m. **$P < 0.01$; ***$P < 0.001$ (ANOVA followed by Bonferroni's test).

© 2013 Nature America, Inc. All rights reserved.

rs12917707 and rs4293393, which are both localized in the *UMOD* promoter. Carriers of the *UMOD* promoter risk variants showed twofold higher *UMOD* expression in kidney samples compared to carriers of the protective haplotype (**Fig. 1b**). We confirmed the association of *UMOD* promoter risk variants with higher uromodulin expression by showing a similar dose-dependent increase in urinary uromodulin levels in a large population-based cohort (SKIPOGH) (**Fig. 1c**). *In silico* analysis revealed that among the lead SNPs from GWAS, rs4293393 maps to a highly conserved region of the *UMOD* promoter (**Supplementary Fig. 1**) and is predicted to lie within a glucocorticoid response element, such that the protective allele would disrupt this element (**Fig. 1d**). We hence tested whether the risk and protective alleles at this SNP affected the transcriptional activity of the human *UMOD* gene promoter. We performed a standard *in vitro* luciferase reporter assay employing a 3.7-kilobase (kb) *UMOD* promoter fragment in three different types of renal cells, including highly differentiated mouse TAL primary cells that retain high *Umod* expression. Notably, the risk allele increased the expression of the luciferase reporter relative to the protective allele by about twofold in each of the types of cells tested (**Fig. 1e**), in accord with the *in vivo* findings. We also confirmed the predicted effect of the rs4293393 risk allele on the promoter response to glucocorticoids (**Supplementary Fig. 2**). The finding that glucocorticoids induced transcription from both constructs is in line with the presence of additional predicted glucocorticoid response elements in the *UMOD* promoter (prediction data not shown) and suggest that uromodulin expression is subject to complex hormonal regulation. Overall, these results demonstrate that the *UMOD* promoter risk variant rs4293393, probably acting together with other variants within the same linkage disequilibrium block, is associated with higher uromodulin expression.

To model this effect *in vivo*, we took advantage of a transgenic mouse line expressing hemagglutinin (HA)-tagged wild-type uromodulin (Tg(Umod)416Lura, here referred to as Tg^{Umodwt} mice). We also generated a line homozygous for the transgene ($Tg^{Umodwt/wt}$ mice). Transgenic animals from both lines were viable, apparently healthy and indistinguishable from control nontransgenic mice (here referred to as control mice). The presence of the transgene caused a dose-dependent increase in uromodulin expression and secretion (**Supplementary Fig. 3a–c**). Notably, uromodulin was expressed at approximately 80% higher amounts in $Tg^{Umodwt/wt}$ mice relative to control mice, comparable to the effect on uromodulin expression in subjects homozygous for *UMOD* risk variants. Similarly to endogenous uromodulin, the transgenic protein was expressed exclusively in TAL segments of the nephron (**Supplementary Fig. 3d–f**; see also ref. 23).

As uromodulin is expressed in the TAL, a tubular segment that has been implicated in rare inherited disorders characterized by defective

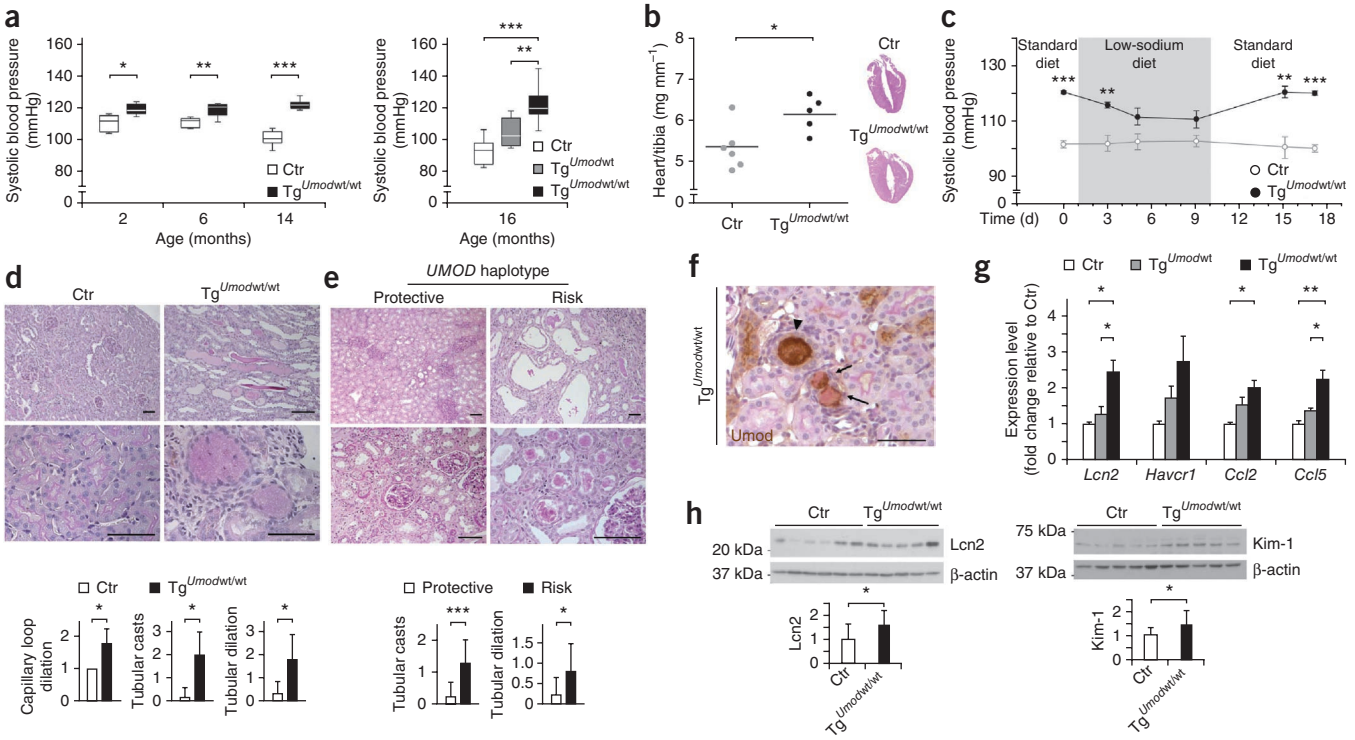

Figure 2 Uromodulin overexpression leads to hypertension and renal damage. (**a**) Box-and-whisker plots showing systolic blood pressure at baseline in control and *Umod* transgenic mice at the indicated ages ($n = 6$–10 mice per group). Bars represent minimum and maximum values. (**b**) Average value and distribution of heart weight relative to tibia length (heart/tibia) in 16-month-old control and $Tg^{Umodwt/wt}$ mice (left) and heart histology showing left ventricular hypertrophy in $Tg^{Umodwt/wt}$ mice (right) (H&E 1× magnification). Each dot represents an individual mouse. (**c**) Average systolic blood pressure in 14-month-old control and $Tg^{Umodwt/wt}$ mice on standard (1% NaCl) or low-sodium (0.01% NaCl) diet ($n = 7$ mice per group). Data are expressed as means ± s.e.m. (**d**) Top, representative renal histological images of 16-month-old control (Ctr) and $Tg^{Umodwt/wt}$ mice. Kidneys from $Tg^{Umodwt/wt}$ mice show numerous dilated tubules (top row) mostly filled by casts (top and bottom rows) (PAS, scale bars, 100 µm). Bottom, quantification of the histological analysis (only parameters reaching statistical significance are shown) ($n = 5$ mice per group). Data are expressed as means ± s.d. (**e**) Top, representative renal tissue from elderly subjects homozygous for the protective or risk variants of rs4293393 and rs12917707. Tissue from individuals homozygous for the protective variants shows normal interstitial compartment (top row) and mild focal tubular damage with increased thickness of the tubular basement membrane (bottom row) ($n = 9$), whereas tissue from subjects homozygous for the risk variants shows dilated tubules with detachment of the tubular epithelium (top row) and presence of tubular casts (bottom row) ($n = 15$) (PAS, scale bars, 100 µm). Bottom, quantification of the histological analysis (only parameters reaching statistical significance are shown). Data are expressed as means ± s.d. (**f**) Tubular casts in renal tissue from a $Tg^{Umodwt/wt}$ mouse are present in TALs (uromodulin-positive) or more distal tubules (uromodulin-negative) and are formed mostly by uromodulin (arrowhead) or by PAS-positive uromodulin-negative (arrows) material. Scale bar, 100 µm. (**g**) Transcript levels (qRT-PCR) of renal damage markers *Lcn2* and *Havcr1* (encoding Kim-1) and chemokines *Ccl2* and *Ccl5* in kidneys from 16-month-old mice ($n = 5$ per group). Data are expressed as means ± s.e.m. (**h**) Representative immunoblot images and quantitative data ($n = 13$ mice per group) showing levels of Lcn2 and Kim-1 in kidney lysates from 16-month-old control and $Tg^{Umodwt/wt}$ mice normalized to the loading control, β-actin. Data are expressed as means ± s.d. $^{*}P < 0.05$; $^{**}P < 0.01$; $^{***}P < 0.001$ determined by unpaired *t*-test (**a** (left), **b**,**c** and **h**), ANOVA followed by Bonferroni's test (**a** (right) and **g**) or Mann-Whitney test (**d** and **e**).

NaCl reabsorption and low blood pressure[10], we first tested whether uromodulin overexpression could affect blood pressure by having an effect on NaCl reabsorption. Blood pressure was indeed markedly higher in transgenic mice relative to control mice in a *Umod* dosage–dependent fashion ($P < 0.0001$, analysis of variance (ANOVA) *post hoc* test for linear trend) (**Fig. 2a**). Blood pressure in $Tg^{Umodwt/wt}$ mice was significantly higher relative to control mice as early as 2 months of age, and the difference in blood pressure increased with age. This age-dependent effect was partly due to low blood pressure in aging control mice, as previously described[24,25] (**Fig. 2a**). High blood pressure in $Tg^{Umodwt/wt}$ mice was associated with a significant increase of the total heart mass and left ventricular hypertrophy, consistent with a chronic hypertensive state (**Fig. 2b**). Hypertension in transgenic mice was salt sensitive, as blood pressure could be normalized to control levels by a low-NaCl diet but returned to elevated levels upon return to a standard NaCl diet (**Fig. 2c**). The changes in dietary salt exposure also caused the expected modifications in aldosterone levels and NaCl handling, which were similar in control and transgenic animals (**Supplementary Fig. 4**).

Transgenic mice had a similar body weight and baseline urine and plasma parameters relative to control mice up to 16 months of age (**Supplementary Table 1** and data not shown). Renal function, as measured by FITC-sinistrin clearance[26], was also normal (**Supplementary Table 1**). However, histological analysis of kidneys from aging $Tg^{Umodwt/wt}$ mice revealed signs of renal damage, mainly localized to and affecting distal segments, with segmental dilation and increased tubular cast area relative to control mice (**Fig. 2d** and Online Methods). We detected similar focal lesions in human nephrectomy samples from individuals older than 65 years of age, and the area of these lesions was increased in individuals homozygous for *UMOD* risk variants relative to those homozygous for protective variants (**Fig. 2e** and Online Methods). Further investigation in $Tg^{Umodwt/wt}$ mice revealed that tubular casts often but not always stained positive for uromodulin and localized to TALs and

© 2013 Nature America, Inc. All rights reserved.

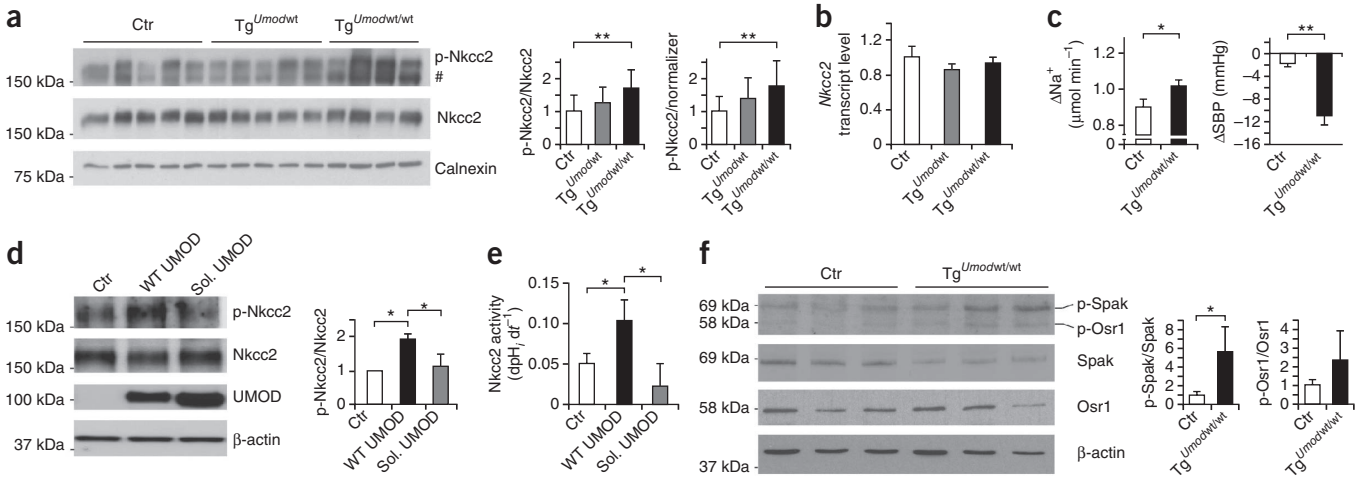

Figure 3 Increased activation of Nkcc2 co-transporter and Spak kinase in Tg$^{Umodwt/wt}$ mice. (**a**) Representative immunoblot images and quantitative data (n = 10–13 mice per group) showing levels of phosphorylated (Thr96 and Thr101) Nkcc2 (p-Nkcc2) and total Nkcc2 in kidney lysates from 16-month-old mice. Data are expressed as means ± s.d. of four independent experiments. #, unspecific signal. Calnexin was used as a loading control. (**b**) *Nkcc2* mRNA (qRT-PCR) in total kidney extracts from 16-month-old mice (n = 5 per group). Data are expressed as means ± s.e.m. (**c**) Change in sodium excretion (left) and systolic blood pressure (SBP, right) in 16-month-old Tg$^{Umodwt/wt}$ and control mice 2 h after treatment with furosemide (n = 8 Ctr mice, n = 6 Tg$^{Umodwt/wt}$ mice (sodium excretion); n = 5 mice per group (SBP)). Data are expressed as means ± s.e.m. (**d**) Representative immunoblot images and quantitative data showing levels of phosphorylated and total Nkcc2 and uromodulin (UMOD) in HEK293 cells stably expressing Nkcc2 and transfected with either wild-type (WT UMOD) or soluble (Sol. UMOD) uromodulin. Ctr, mock transfected cells. β-actin was used as a loading control. Densitometric analysis (means ± s.d. of three independent experiments) is shown. (**e**) Quantification of Nkcc2 activity as assessed by $dpH_i\ dt^{-1}$. Data are from eight independent experiments and are expressed as means ± s.e.m. (**f**) Representative immunoblot images and quantitative data (n = 4 mice per group) showing levels of phosphorylated and total Spak and Osr1 in kidney lysates from 16 month-old control and Tg$^{Umodwt/wt}$ mice. Bars indicate means ± s.d. *P < 0.05; **P < 0.01 determined by ANOVA followed by Bonferroni's test (**a**,**b**,**d** and **e**) or unpaired t test (**c** and **f**).

more distal segments (**Fig. 2f**). Evidence of renal damage in transgenic mice also included increased renal expression of established markers of tubule damage (*Lcn2*, encoding lipocalin 2 (Lcn2), and *Havcr1*, encoding kidney injury molecule-1 (Kim-1)) and the chemokines *Ccl2* and *Ccl5* (**Fig. 2g**,**h**), and transgenic mice also had substantial microalbuminuria (data not shown). There was also a significant dilation of glomerular capillary loops in these mice (**Fig. 2d** and **Supplementary Fig. 5a**). There were no signs of interstitial vascular remodeling in the kidney that could be ascribed to chronic hypertension (**Supplementary Fig. 5b**), in line with the fairly rapid BP response induced by changes in dietary salt (see above).

In the context of the normal renal function of *Umod* transgenic mice, which showed normal or slightly decreased renin expression (**Supplementary Fig. 6**), we hypothesized that the salt-sensitive hypertension of the transgenic mice could be caused by abnormal activation of Nkcc2, the main sodium transporter in the TAL. Consistent with this hypothesis, we found a significantly higher level of phosphorylation on Nkcc2 at activating sites (Thr96 and Thr101)[27,28] in Tg$^{Umodwt/wt}$ mice relative to control mice (**Fig. 3a**). The increase in phosphorylated Nkcc2 levels was linearly correlated with *Umod* gene dosage (P < 0.01, ANOVA *post hoc* test for linear trend). The specificity of this effect for phosphorylation on Nkcc2, rather than on Nkcc1, which can also be recognized by the antibodies used in this experiment, is supported by the almost exclusive localization of the phosphorylated protein signal on the apical membrane of TAL cells, which lacks Nkcc1, and by the 40-fold higher global expression of *Nkcc2* as compared to *Nkcc1* in the kidney (**Supplementary Fig. 7a**,**b**). In line with a post-translational mechanism for the regulation of Nkcc2, *Nkcc2* transcript levels were not different between transgenic and control mice (**Fig. 3b**). Romk expression and membrane localization were similar in transgenic and control mice (**Supplementary Fig. 8a–c**).

To test the functional importance of Nkcc2 to the hypertensive phenotype of *Umod* transgenic mice, we assessed the response of these mice to furosemide, a loop diuretic that specifically targets NKCC2. Treatment of Tg$^{Umodwt/wt}$ mice with a single dose of furosemide induced both a significantly enhanced natriuretic effect and a significant reduction of blood pressure (**Fig. 3c**). The enhanced response of transgenic mice compared to control mice to furosemide treatment is probably due to increased Nkcc2 activity and increased sodium reabsorption in the TAL rather than to adaptive downregulation of NaCl reabsorption in more distal nephron segments, as control and transgenic mice had comparable levels of sodium-chloride symporter (Ncc) (distal convoluted tubules) and epithelial sodium channel (ENaC) (collecting ducts) (**Supplementary Fig. 8d**,**e**), as well as similar levels of aldosterone (**Supplementary Fig. 4b**).

We next investigated the direct effect of uromodulin on Nkcc2 activation in kidney cells stably expressing Nkcc2 and transiently transfected with either human wild-type uromodulin or with a soluble uromodulin isoform truncated at the glycosylphosphatidylinositol (GPI)-anchoring site (S614X)[29]. Expression of wild-type uromodulin led to a significant increase in Nkcc2 phosphorylation that correlated with an increase in its activity (**Fig. 3d**,**e**). The effect on Nkcc2 phosphorylation and activity was completely lost in cells transfected with soluble uromodulin. These findings confirm in a mammalian system the previously described effect of uromodulin on NKCC2 phosphorylation and activity[19] and strongly suggest that this effect is exerted by membrane-anchored uromodulin.

NKCC2 phosphorylation is, at least in part, mediated by STE20/SPS1-related proline-alanine–rich kinase (SPAK) and by oxidative stress response 1 kinase (OSR1)[30,31]. The level of Spak phosphorylated at Thr243 (i.e., active Spak) relative to total Spak was significantly increased in Tg$^{Umodwt/wt}$ mice compared to control mice, and there was also a trend towards an increase in the level of phosphorylated Osr1 (at Thr185) relative to total Osr1 in Tg$^{Umodwt/wt}$ mice (**Fig. 3f** and **Supplementary Fig. 7c**). These data demonstrate upregulation of this regulatory network by uromodulin overexpression. Consistent with this effect, the transcript level of kidney-specific *Spak*, an isoform

© 2013 Nature America, Inc. All rights reserved.

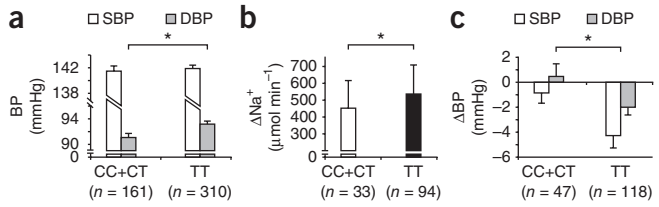

Figure 4 Increased blood pressure and response to furosemide in hypertensive patients homozygous for *UMOD* risk variants. (**a**) Average values for systolic (SBP) and diastolic (DBP) blood pressure in individuals homozygous for the rs4293393 risk genotype (TT) and for individuals either homozygous for the protective genotype or heterozygous (CC + CT), as assessed by 24-h ambulatory blood pressure monitoring. (**b**,**c**) Response to furosemide treatment in hypertensive patients with the indicated rs4293393 genotypes. Changes in sodium excretion (**b**) and SBP and DBP (**c**) 4 h after treatment are shown. Data are expressed as means ± s.e.m. (**a** and **c**) or means ± s.d. (**b**). $^*P < 0.05$ (ANOVA).

which is expressed mainly in the TAL and which acts as a negative regulator of Nkcc2 phosphorylation[32], but not that of full-length *Spak*, was reduced in transgenic mice (**Supplementary Fig. 7d**,**e**).

Finally, to investigate whether *UMOD* variants could have a role in modulating blood pressure in humans, we took advantage of a well-characterized cohort of naive (never-treated) hypertensive subjects (MI_HPT cohort) stratified *a posteriori* for their rs4293393 SNP status (**Supplementary Table 2**). Baseline mean diastolic blood pressure was significantly higher in hypertensive individuals homozygous for the risk allele relative to individuals that were heterozygous or were homozygous for the protective allele (**Fig. 4a**). For a subset of these subjects, data from furosemide tests were also available. Patients homozygous for the risk allele showed an increased diuretic response,with a significantly higher increase of natriuresis over baseline values (**Fig. 4b**) and a more marked drop in blood pressure, with a significant difference in the decrease of DBP and a similar trend for SBP ($P = 0.06$) (**Fig. 4c** and **Supplementary Table 2**). Despite the limitations of this study, which involved retrospective analysis of a relatively small-sized cohort, these results suggest that the mechanism causing hypertension in transgenic mice (i.e., increased NKCC2 activity linked to overexpression of uromodulin) may contribute to hypertension in humans.

This work identifies a causal role for a major risk locus for CKD and hypertension, which had been identified in multiple GWAS. Studies of rare monogenic disorders[33] have contributed considerably to our current knowledge of the functional relationship between NaCl handling in the kidney and blood pressure regulation. Loss-of-function mutations impairing sodium reabsorption have been associated with salt wasting and reduced blood pressure in monogenic diseases affecting the TAL (Bartter's syndrome) or more distal segments (Gitelman's syndrome and pseudohypoaldosteronism type 1). Thus far, increased sodium reabsorption leading to hypertension has been linked exclusively to mutations affecting these more distal segments (Liddle's syndrome and pseudohypoaldosteronism type 2)[10,14]. The new gain-of-function mechanism described here completes the paradigm that links renal transport of NaCl with blood pressure regulation. This mechanism could be widely relevant to human hypertension, given the high frequency of *UMOD* risk variants in the general population (**Supplementary Table 3**). Further prospective studies will be necessary to confirm our findings in patients with hypertension and to elucidate the contribution of increased sodium transport in the TAL to hypertension.

Through evidence obtained in mouse and cellular models, this study establishes the importance of uromodulin in modulating NaCl handling in the TAL. Notably, both the expression and urinary excretion of uromodulin are increased by high sodium intake in rats[34] and humans[35]. Here, we demonstrate that *UMOD* promoter activity is modulated by glucocorticoids, which are known to have a central role in ion homeostasis and blood pressure regulation and have been shown to act on TAL cells[36].

Both in aging $Tg^{Umod\text{wt/wt}}$ mice and in elderly individuals homozygous for *UMOD* promoter risk variants, upregulation of uromodulin expression was associated with the presence of focal renal lesions, tubular dilation and casts, despite normal kidney function. The focal kidney damage observed in $Tg^{Umod\text{wt/wt}}$ mice seems unlikely to be secondary to chronic hypertension, as no such lesions were detected in other rodent models of hypertension[37]. Rather, these lesions, as well as the upregulation of Lcn2 and Kim-1 expression, are reminiscent of changes observed in aging kidneys[38,39]. These results suggest that uromodulin overexpression is unlikely to lead to renal failure *per se*, but could predispose to CKD. In this scenario, CKD, whose incidence increases with age, would be triggered by additional conditions harming the kidney. This hypothesis is supported by recent evidence that the association of *UMOD* promoter risk variants with CKD is stronger in the older age groups with additional comorbid conditions[7,9].

Our study shows that common variants in a gene associated with a rare monogenic disorder may play a causal role in complex traits in the general population. *UMOD* risk variants are present in a high frequency in all ethnic groups studied (**Supplementary Table 3**), suggesting the action of selective pressure. Selective pressure for a disease-associated variant is atypical but not unprecedented; for example, *APOL1* variants are strongly associated with kidney disease in African Americans but increase resistance to *Trypanosoma brucei rhodesiense* infection[40]. We speculate that selective pressure might have favored *UMOD* variants leading to high expression and urinary levels of uromodulin due to its protective effect in urinary tract infections and its stimulation of renal salt reabsorption. However, with increased life expectancy, better hygienic conditions and higher salt intake, these same variants could now be exerting a deleterious effect. Accordingly, therapies targeting uromodulin expression or function may be relevant for controlling blood pressure and preserving renal function.

METHODS

Methods and any associated references are available in the online version of the paper.

Note: Any Supplementary Information and Source Data files are available in the online version of the paper.

ACKNOWLEDGMENTS

We thank M. Azizi, A. Blanchard, G. Capasso, M. Carrel, Y. Cnops, A. Creatore, S. Delli Carpini, P. Houillier, X. Jeunemaitre, R. Latini, N. Morel, S. Terryn and S. Youhanna for help, technical assistance and fruitful discussions. We are grateful to S. Bourgeois (University of Zurich) for providing MKTAL cells, to D. Alessi (University of Dundee) for antibodies to SPAK and phospho-SPAK/OSR1, to B. Forbush (Yale University) for antibody to phospho-NKCC2 and to D. Schock-Kusch and N. Gretz (University of Heidelberg) for FITC-sinistrin clearance reagents and technical assistance. This work was supported by Telethon-Italy (TCR08006), the Italian Ministry of Health (grant RF-2010-2319394), Associazione per il Bambino Nefropatico, the Belgian Fonds National de la Recherche Scientifique and Fonds pour la Recherche Scientifique Médicale, a Concerted Research Action (10/15-029), an Interuniversity Attraction Pole program initiated by the Belgian Science Policy Office, the Gebert Rüf Stiftung (Project GRS-038/12), the National Centre of Competence in Research Kidney. CH (Swiss National Science Foundation), the Swiss National Science Foundation project grant 310030_146490 and the European Community's Seventh Framework Programme (FP7/2007-2013) under grant agreement 246539 (Marie Curie) and grant 305608 (EURenOmics). The SKIPOGH project is funded by the Swiss National Science Foundation (33CM30-124087/1 and 33CM30_140331). L.R. is an Associate Telethon Scientist.

© 2013 Nature America, Inc. All rights reserved.

AUTHOR CONTRIBUTIONS
M.T. and S.J. characterized the mouse model and carried out immunofluorescence and immunoblot analyses on mouse tissue; J.L. carried out expression studies for salt transporters; M.T. and C.S. performed RNA extraction and qRT-PCR analysis on mouse and human kidneys; M.T., S.J. and G.R. performed blood pressure measurements; S.J. and H.D. carried out plasma and urine analyses on mice; L.R., H.D. and M.T. did bioinformatics analysis; H.D. carried out *in vitro* analysis on the *UMOD* promoter; B.G. performed studies based on primary TAL cells. The SKIPOGH investigators provided the population-based cohort used for urinary uromodulin determination (H.D. and O.D.); P.M., C.L. and F.T. contributed to the hypertensive patient (MI_HPT) cohort patient recruitment and assessment; P.M. and C.L. designed and performed the study on human hypertensive patients; L.C. performed DNA extraction and genotyping on human samples; K.L. contributed in designing the *in vitro* experiments on Nkcc2 phosphorylation and activity that were performed by S.D.; G.D.A. and M.P.R. supervised the histology work on mouse and human kidneys; G.D.A., M.P.R. and M.I. carried out histological assessment; M.T. and M.I. performed histological and immunohistochemistry staining; L.R. and O.D. designed the study and supervised the experiments; L.R., O.D. and M.T. wrote the manuscript. All authors critically reviewed and approved the manuscript.

COMPETING FINANCIAL INTERESTS
The authors declare no competing financial interests.

Reprints and permissions information is available online at http://www.nature.com/reprints/index.html.

© 2013 Nature America, Inc. All rights reserved.

1. Kearney, P.M. *et al.* Global burden of hypertension: analysis of worldwide data. *Lancet* **365**, 217–223 (2005).
2. Levey, A.S. *et al.* Chronic kidney disease as a global public health problem: approaches and initiatives–a position statement from Kidney Disease Improving Global Outcomes. *Kidney Int.* **72**, 247–259 (2007).
3. Padmanabhan, S. *et al.* Genome-wide association study of blood pressure extremes identifies variant near UMOD associated with hypertension. *PLoS Genet.* **6**, e1001177 (2010).
4. Köttgen, A. *et al.* Multiple loci associated with indices of renal function and chronic kidney disease. *Nat. Genet.* **41**, 712–717 (2009).
5. Köttgen, A. *et al.* New loci associated with kidney function and chronic kidney disease. *Nat. Genet.* **42**, 376–384 (2010).
6. Pattaro, C. *et al.* A meta-analysis of genome-wide data from five European isolates reveals an association of COL22A1, SYT1, and GABRR2 with serum creatinine level. *BMC Med. Genet.* **11**, 41 (2010).
7. Gudbjartsson, D.F. *et al.* Association of variants at UMOD with chronic kidney disease and kidney stones-role of age and comorbid diseases. *PLoS Genet.* **6**, e1001039 (2010).
8. Böger, C.A. *et al.* Association of eGFR-related loci identified by GWAS with incident CKD and ESRD. *PLoS Genet.* **7**, e1002292 (2011).
9. Pattaro, C. *et al.* Genome-wide association and functional follow-up reveals new loci for kidney function. *PLoS Genet.* **8**, e1002584 (2012).
10. Lifton, R.P., Gharavi, A.G. & Geller, D.S. Molecular mechanisms of human hypertension. *Cell* **104**, 545–556 (2001).
11. Boyden, L.M. *et al.* Mutations in kelch-like 3 and cullin 3 cause hypertension and electrolyte abnormalities. *Nature* **482**, 98–102 (2012).
12. Eckardt, K.U. *et al.* Evolving importance of kidney disease: from subspecialty to global health burden. *Lancet* **382**, 158–169 (2013).
13. O'Seaghdha, C.M. & Fox, C.S. Genome-wide association studies of chronic kidney disease: what have we learned? *Nat. Rev. Nephrol.* **8**, 89–99 (2012).
14. Padmanabhan, S., Newton-Cheh, C. & Dominiczak, A.F. Genetic basis of blood pressure and hypertension. *Trends Genet.* **28**, 397–408 (2012).
15. Rampoldi, L., Scolari, F., Amoroso, A., Ghiggeri, G. & Devuyst, O. The rediscovery of uromodulin (Tamm-Horsfall protein): from tubulointerstitial nephropathy to chronic kidney disease. *Kidney Int.* **80**, 338–347 (2011).
16. Bates, J.M. *et al.* Tamm-Horsfall protein knockout mice are more prone to urinary tract infection: rapid communication. *Kidney Int.* **65**, 791–797 (2004).
17. Liu, Y. *et al.* Progressive renal papillary calcification and ureteral stone formation in mice deficient for Tamm-Horsfall protein. *Am. J. Physiol. Renal Physiol.* **299**, F469–F478 (2010).
18. Bachmann, S. *et al.* Renal effects of Tamm-Horsfall protein (uromodulin) deficiency in mice. *Am. J. Physiol. Renal Physiol.* **288**, F559–F567 (2005).
19. Mutig, K. *et al.* Activation of the bumetanide-sensitive Na^+,K^+,$2Cl^-$ cotransporter (NKCC2) is facilitated by Tamm-Horsfall protein in a chloride-sensitive manner. *J. Biol. Chem.* **286**, 30200–30210 (2011).
20. Renigunta, A. *et al.* Tamm-Horsfall glycoprotein interacts with renal outer medullary potassium channel ROMK2 and regulates its function. *J. Biol. Chem.* **286**, 2224–2235 (2011).
21. Hart, T.C. *et al.* Mutations of the *UMOD* gene are responsible for medullary cystic kidney disease 2 and familial juvenile hyperuricaemic nephropathy. *J. Med. Genet.* **39**, 882–892 (2002).
22. Eddy, A.A. Scraping fibrosis: UMODulating renal fibrosis. *Nat. Med.* **17**, 553–555 (2011).
23. Bernascone, I. *et al.* A transgenic mouse model for uromodulin-associated kidney diseases shows specific tubulo-interstitial damage, urinary concentrating defect and renal failure. *Hum. Mol. Genet.* **19**, 2998–3010 (2010).
24. Simpson, R.U., Hershey, S.H. & Nibbelink, K.A. Characterization of heart size and blood pressure in the vitamin D receptor knockout mouse. *J. Steroid Biochem. Mol. Biol.* **103**, 521–524 (2007).
25. Han, J. *et al.* Age-related changes in blood pressure in the senescence-accelerated mouse (SAM): aged SAMP1 mice manifest hypertensive vascular disease. *Lab. Anim. Sci.* **48**, 256–263 (1998).
26. Schreiber, A. *et al.* Transcutaneous measurement of renal function in conscious mice. *Am. J. Physiol. Renal Physiol.* **303**, F783–F788 (2012).
27. Giménez, I. & Forbush, B. Regulatory phosphorylation sites in the NH2 terminus of the renal Na-K-Cl cotransporter (NKCC2). *Am. J. Physiol. Renal Physiol.* **289**, F1341–F1345 (2005).
28. Ponce-Coria, J. *et al.* Regulation of NKCC2 by a chloride-sensing mechanism involving the WNK3 and SPAK kinases. *Proc. Natl. Acad. Sci. USA* **105**, 8458–8463 (2008).
29. Schaeffer, C., Santambrogio, S., Perucca, S., Casari, G. & Rampoldi, L. Analysis of uromodulin polymerization provides new insights into the mechanisms regulating ZP domain-mediated protein assembly. *Mol. Biol. Cell* **20**, 589–599 (2009).
30. Piechotta, K., Lu, J. & Delpire, E. Cation chloride cotransporters interact with the stress-related kinases Ste20-related proline-alanine-rich kinase (SPAK) and oxidative stress response 1 (OSR1). *J. Biol. Chem.* **277**, 50812–50819 (2002).
31. Richardson, C. *et al.* Regulation of the NKCC2 ion cotransporter by SPAK-OSR1-dependent and -independent pathways. *J. Cell Sci.* **124**, 789–800 (2011).
32. McCormick, J.A. *et al.* A SPAK isoform switch modulates renal salt transport and blood pressure. *Cell Metab.* **14**, 352–364 (2011).
33. Devuyst, O. Salt wasting and blood pressure. *Nat. Genet.* **40**, 495–496 (2008).
34. Ying, W.Z. & Sanders, P.W. Dietary salt regulates expression of Tamm-Horsfall glycoprotein in rats. *Kidney Int.* **54**, 1150–1156 (1998).
35. Torffvit, O., Melander, O. & Hulten, U.L. Urinary excretion rate of Tamm-Horsfall protein is related to salt intake in humans. *Nephron Physiol.* **97**, 31–36 (2004).
36. Stubbe, J., Madsen, K., Nielsen, F.T., Skott, O. & Jensen, B.L. Glucocorticoid impairs growth of kidney outer medulla and accelerates loop of Henle differentiation and urinary concentrating capacity in rat kidney development. *Am. J. Physiol. Renal Physiol.* **291**, F812–F822 (2006).
37. Ferrandi, M. *et al.* α- and β-adducin polymorphisms affect podocyte proteins and proteinuria in rodents and decline of renal function in human IgA nephropathy. *J. Mol. Med.* **88**, 203–217 (2010).
38. Mulder, W.J. & Hillen, H.F. Renal function and renal disease in the elderly: Part I. *Eur. J. Intern. Med.* **12**, 86–97 (2001).
39. Chen, G. *et al.* Increased susceptibility of aging kidney to ischemic injury: identification of candidate genes changed during aging, but corrected by caloric restriction. *Am. J. Physiol. Renal Physiol.* **293**, F1272–F1281 (2007).
40. Genovese, G. *et al.* Association of trypanolytic ApoL1 variants with kidney disease in African Americans. *Science* **329**, 841–845 (2010).

The SKIPOGH team

Murielle Bochud[14], Michel Burnier[15], Olivier Devuyst[2], Pierre-Yves Martin[16], Markus Mohaupt[17], Fred Paccaud[14], Antoinette Pechère-Bertschi[18], Bruno Vogt[17], Daniel Ackermann[17], Georg Ehret[19], Idris Guessous[12,20], Belen Ponte[16] & Menno Pruijm[15]

[14]Institute of Social and Preventive Medicine, Lausanne University Hospital, Lausanne, Switzerland. [15]Department of Nephrology, Lausanne University Hospital, Lausanne, Switzerland. [16]Department of Nephrology, Geneva University Hospitals, Geneva, Switzerland. [17]Department of Nephrology, Hypertension and Clinical Pharmacology, Inselspital, University Hospital and University of Bern, Bern, Switzerland. [18]Hypertension Unit, Geneva University Hospitals, Geneva, Switzerland. [19]Cardiology, Department of Specialties of Internal Medicine, Geneva University Hospitals, Geneva, Switzerland. [20]Unit of Population Epidemiology, Division of Primary Care Medicine, Department of Community Medicine and Primary Care and Emergency Medicine, Geneva University Hospitals, Geneva, Switzerland.

ONLINE METHODS

MI_HPT cohort. The MI_HPT cohort study was approved by the Comitato Etico Ospedale San Raffaele, the ethical committee of the San Raffaele Hospital. All participants provided informed written consent.

In this study, we enrolled a cohort of 471 (391 males and 80 females) never-treated hypertensive patients referred to the Outpatient Clinic at San Raffaele Hospital[41]. Patients were between 20 and 65 years old and each had a body mass index <30 kg/m^2 and systolic and diastolic blood pressure (SBP/DBP) >140/90 mm Hg and <160/110 mm Hg. We excluded from the study patients with chronic or acute pathologies, clinical history for ischemic cardiomyopathy, cardiac decompensation, cerebral vasculopathy, creatinine clearance <80 ml min^{-1}, liver failure, diabetes, severe essential hypertension or secondary arterial hypertension. We also excluded subjects under antihypertensive or estrogen or progestin therapy or with a history of addiction and/or alcohol abuse. We gave patients dietary instructions including a list of suggested and forbidden foods and verified compliancy by assessing 24-h urinary sodium excretion.

SKIPOGH cohort. The Swiss Kidney Project on Genes in Hypertension (SKIPOGH) study was approved by Commission d'éthique de la recherche clinique, the ethical committee of Lausanne University Hospital, the Commission centrale d'éthique, the ethical committee of Geneva University Hospitals and the Kantonale Ethikkommission Bern, the ethical committee of University Hospital of Bern (Inselspital). All participants provided informed written consent.

The SKIPOGH study is a family-based cross-sectional study exploring the role of genes in blood pressure and kidney function regulation. We recruited participants from December 2009 until April 2013 in three centers (Bern, Geneva and Lausanne in Switzerland), as previously described[42]. Participants collected urine during the daytime, which had a median duration of 16 h (interquartile range, 2). The analysis of uromodulin urinary levels was performed for all available samples.

Human kidney samples. The study on adult human kidney samples was approved by the Comitato Etico Ospedale San Raffaele, the ethical committee of the San Raffaele Hospital. All participants provided informed written consent. Human renal samples were from individuals who underwent nephrectomy at the San Raffaele Hospital because of renal carcinoma. Samples of normal tissue were dissected, fixed in 4% buffered formaldehyde, embedded in paraffin and subsequently cut into 3-µm sections for histology. Tissue samples were stored in RNAlater (Qiagen) at −80 °C for molecular analysis. Only kidneys from patients with normal renal function (i.e., eGFR > 90 ml min^{-1}, calculated by using the four-variable Modification of Diet in Renal Disease formula[43]) and from patients not under antitumor treatment at the time of explant were eligible for this study. We matched individuals homozygous for the rs12917707 and rs4293393 protective alleles (n = 17; 41.2% females; age at the time of nephrectomy 67.7 ± 12.7 years) for age and sex with at least one individual homozygous for the risk alleles (n = 27; 33.3% females; age at the time of nephrectomy 67.9 ± 9.6 years).

Genotyping. We carried out genotyping in individuals in the MI_HPT cohort and in individuals who underwent nephrectomy on genomic DNA extracted from blood samples or renal tissue, respectively. We used the QIAamp DNA Mini Kit (Qiagen) and carried out 5′ nuclease allelic discrimination assays with allele-specific MGB probes (TaqMan, Applied Biosystems) for marker SNPs rs4293393 (Assay ID C__27865986_10) and rs12917707 (Assay ID C__31122302_10) according to manufacturer's instructions (call rate of 97.2%).

Genotyping of SNP rs4293393 in individuals in the SKIPOGH cohort was performed on genomic DNA extracted from white blood cells at LGC Genomics (formerly KBioscience) using the Competitive Allele Specific PCR technique (KASPar v4.0) (call rate of 96.4%). Additional quality-control criteria included inter- and intraplate duplicate testing and clear separation of signal clusters.

A reproducibility test on randomly selected duplicates (10% in the MI_HPT and 4.5% in the SKIPOGH cohorts) showed 100% concordance. The frequency of the rs4293393 minor allele C was 0.180 in the MI_HPT cohort and 0.163 in the SKIPOGH cohort. The P values for Hardy-Weinberg equilibrium were 0.048 (MI_HPT) and 0.34 (SKIPOGH). The deviation in the MI_HPT cohort was driven by underrepresentation of individuals homozygous for the protective allele C (observed 9 versus expected 15.3). This finding is in line with GWAS showing association of the risk allele T with hypertension[3].

Patient ambulatory blood pressure monitoring and furosemide test. Patients in the MI_HPT cohort (n = 471) underwent 24-h ambulatory blood pressure monitoring (Spacelab 90207; Spacelab Medical) on a day chosen for typical weekly activity. Recordings were performed every 10 min during waking hours (daytime) and every 30 min during nighttime.

Owing to the low frequency of the rs4293393 protective allele, we grouped patients carrying one (CT, n = 152) or two (CC, n = 9) copies of the protective variant and compared them with those homozygous for the risk variant (TT, n = 310). The two groups did not significantly differ by age, sex, BMI or renal function (see **Supplementary Table 2**).

A subgroup of 165 patients underwent a furosemide test, as follows. After 2 h equilibration, we orally administered 25 mg of furosemide (Sanofi-Aventis). We collected urine immediately before and 4 h after furosemide administration. We measured BP every 60 min during the equilibration period and every 30 min after furosemide treatment. Reported values are the average of three measurements done every minute at each of the timepoints. As for ambulatory blood pressure monitoring, we grouped patients carrying one (CT, n = 44) or two (CC, n = 3) copies of the protective variant and compared them with homozygous for the risk variant (TT, n = 118). The two groups did not significantly differ in age, sex, BMI or renal function.

We measured urinary Na^+ by flame photometry, creatinine by picric acid test and plasma renin activity by commercial radioimmunoassay (Sorin Laboratories).

Human urinary uromodulin measurements. We measured urinary uromodulin concentration by ELISA using on a sheep anti-human uromodulin antibody (Meridian Life Science, K90071C, 5 µg ml^{-1}) as the capture antibody, a mouse monoclonal anti-human THP antibody (Cedarlane, CL1032A, 1 µg ml^{-1}) as the primary antibody and a goat anti-mouse IgG (H+L) horseradish peroxidase–conjugated antibody (BioRad, 1721011, 1:2,000) as the secondary antibody[44]. We used human uromodulin (Millipore, stock solution 100 µg ml^{-1}) to establish the standard curve[45]. The uromodulin ELISA assay had a sensitivity of 2.8 ng ml^{-1}, a linearity of 1.0, an interassay variability of 3.3% and an intra-assay variability of 5.5% . We measured urinary creatinine levels using Beckman Coulter Synchron System Creatinine Assay (Unicell DxC Synchron Clinical System)[46] following the manufacturer's instructions. We normalized uromodulin concentration to creatinine concentration (uromodulin-to-creatinine ratio) to compensate for variations in urine concentration.

Transgenic mice. We generated Tg$^{Umod\text{wt}}$ mice as described previously[23]. Briefly, we injected the FVB/N mouse strain with the transgenic uromodulin construct composed of a 2.9-kb fragment of the *Umod* gene promoter, the first noncoding exon, the first intron, the coding sequence from exon 2 to 11 and the entire 3′ untranslated region. An HA tag was inserted at the uromodulin N terminus. We generated Tg$^{Umod\text{wt/wt}}$ mice by breeding Tg$^{Umod\text{wt}}$ mice and verified transgene homozygosity by Southern blot analysis. The two transgenic lines are in pure FVB/N background. Control mice were nontransgenic animals in the same isogenic background. We carried out all animal procedures on female mice at San Raffaele Scientific Institute, Milan, Italy, and at Université Catholique de Louvain, Brussels, Belgium, according to protocols approved by the San Raffaele Institutional Animal Care and Use Committee and by the Belgian National Research Council Guide for the Care and Use of Laboratory Animals/Animal Ethics Committee, respectively.

Plasma and urine collection and analysis. We obtained urine and plasma from age- and gender-matched transgenic and control mice. Mice were housed in a light- and temperature-controlled room with *ad libitum* access to tap water and standard chow (Diet AO3, SAFE; 25/18 GR Mucedola Srl) or low-sodium chow (E15430-24, SSNIFF). We collected urine using individual metabolic cages (14 h overnight for baseline measurement and 2 h after furosemide administration, 10 mg per kg body weight) after appropriate training of the mice. We obtained blood by venous puncture or at the time of killing by decapitation. Sampling procedures were identical in all groups. We measured urinary electrolytes, creatinine and albumin, plasma electrolytes, creatinine (enzymatic determination), urea and uric acid on a Synchron CX5 analyzer (Beckman Coulter) and measured aldosterone using a validated Aldosterone

© 2013 Nature America, Inc. All rights reserved.

EIA kit (Cayman Chemical) according to the manufacturer's instructions and normalizing to urinary creatinine (Beckman Coulter Synchron System Creatinine Assay). We measured osmolality on a Fiske osmometer (Advanced Instruments).

Mouse blood pressure measurements. We measured systolic BP by the tail-cuff method (Physiograph Narco or BP-2000, Visitech Systems) on two different days in conscious animals after appropriate training of the mice. We averaged four to six successive measurements.

Tissue collection and preparation. To collect organs (kidney, heart, spleen, brain, adrenal glands, aorta and testis), the mice were killed by decapitation or cervical dislocation after anesthesia with Sevoflurane (Abbott). We immediately homogenized organs for protein or RNA extraction. We fixed renal and cardiac tissue in 4% paraformaldehyde before embedding in paraffin for histological, immunohistochemical and immunofluorescence analysis.

Cell cultures. We maintained human embryonic kidney (HEK) 293 cells in DMEM supplemented with 10% FBS (Invitrogen) and 1% penicillin/streptomycin. MKTAL cells are an immortalized TAL line isolated and characterized by Bourgeois *et al.*[47]. We cultured MKTAL cells in DMEM:F12 (1:1) with the SingleQuots Kit (Lonza) containing hydrocortisone, hEGF, FBS, epinephrine, insulin, triiodothyronine, transferrin and gentamicin/amphotericin. We obtained TAL primary cultures (mTAL) from microdissected tubules of the outer medulla of 5-week-old collagenase-treated C57BL/6 mouse kidneys according to the method described by Terryn *et al.*[48]. We selected TAL tubules on the basis of their morphology[49] and cultured them on permeable filter supports for 14 d, allowing the formation of well-polarized confluent monolayers. These monolayers are characterized by morphological, functional and structural properties similar to those of the TAL segment *in vivo*, including a high level of endogenous uromodulin expression[49]. We kept cells at 37 °C in a humidified atmosphere containing 5% CO_2.

Constructs. We cloned a 3.7-kb fragment of the human *UMOD* gene promoter containing the risk allele at the SNP rs4293393 (nucleotide −551 T) into the pGL3-Basic Luciferase Reporter vector (Promega) in two steps. We obtained the promoter region from nucleotide +1 to −1092 by PCR using primers with MluI (forward, 5′-TTACGCGTCACGTTGTGCACTTGTACCC-3′) and XhoI (reverse, 5′-TCTCGAGTGGTCATGATGTGCCTCATAC-3′) tails, and the promoter region from nucleotide −1093 to −3684 by PCR using primers with SacI (forward, 5′-TTGAGCTCATTCAGGACACGGTGTAAGG-3′) and MluI (reverse, 5′-TTACGCGTCAGGTTTGTTACATATGTATAC-3′) tails. We generated the promoter construct containing the rs4293393 protective allele (nucleotide −551 C) by site-directed mutagenesis using the QuickChange Lightning Site-Directed Mutagenesis Kit (Stratagene, Agilent) following the manufacturer's protocol. We confirmed all plasmids by sequencing.

We cloned HA-tagged human wild-type uromodulin (WT UMOD) and truncated uromodulin soluble isoform (Sol. UMOD), which lacks the GPI-anchoring site (S614X), into the expression vector pcDNA3.1 (+) (Invitrogen), as previously described[29].

***UMOD* promoter activity *in vitro*.** We tested the effect of rs4293393 protective and risk alleles on the transcriptional activity of the *UMOD* promoter in mTAL, MKTAL and HEK293 cells. Whereas mTAL cells retain high uromodulin expression consistent with their fully differentiated state, weak or no uromodulin expression was detected in MKTAL and HEK293 cells, respectively (qRT-PCR, data not shown).

We transiently transfected mTAL, MKTAL and HEK293 cells with 2 μg of a firefly luciferase reporter plasmid (pGL3-Basic, Promega), either promoterless or carrying *UMOD* promoter fragments (see constructs paragraph) and 10 ng of a *Renilla* luciferase vector (pRL-SV40, Promega) using Lipofectamine 2000 (Invitrogen) according to manufacturer's instructions.

We evaluated luciferase activity 48 h after transfection with the Dual-Luciferase Reporter Assay System (Promega) using a GloMax 96 luminometer (Promega) with 10 s of integration time (the duration of measurement per well). Firefly luciferase activity was corrected for transfection efficiency using measurement of *Renilla* luciferase activity. We used the promoterless pGL3-Basic vector as a negative control. To assess the response of the *UMOD* promoter to glucocorticoids, 24 h after transfection cells were treated with 1 μM dexamethasone (Sigma) and/or 10 μM RU-486 (Sigma) for 48 h. For each combination of *UMOD* allele and cell type, we carried out at least four independent transfections and assayed extracts in duplicate.

Nkcc2 cotransporter activity *in vitro*. We cloned a construct containing a cDNA for mouse Nkcc2 with a Myc tag fused to its N-terminus into the pTarget expression vector (Promega). To generate HEK293 cells stably expressing Nkcc2, we transfected the cells, selected for resistance to geneticin (G418, 500 μg ml^{-1}) and isolated single clones. We performed all experiments on the same clone. We carried out transient transfection of plasmids expressing full-length or truncated uromodulin or empty vector using Lipofectamine and Plus Reagent (Invitrogen) according to the manufacturer's instructions. Equal expression of the two transfected uromodulin isoforms was verified by qRT-PCR (data not shown).

We measured Nkcc2 cotransport activity as bumetanide-sensitive NH_4 influx as previously described[50]. Briefly, we used the intracellularly trapped pH-sensitive dye BCECF to measured cytoplasmic pH (pH_i) in cells grown to confluence on coverslips. We measured baseline pH_i in cells bathed at 37 °C in a CO_2-free Hepes-Tris buffered medium. We then added NH_4Cl (20 mM) to the medium to induce cellular alkalinization and measured the initial rate of intracellular pH recovery ($dpH_i\ dt^{-1}$) over the first 20 s of recording. We used the dpH_i caused by NH_4Cl addition to calculate the cell buffer capacity. Nkcc2 cotransporter activity is therefore expressed as $dpH_i\ dt^{-1}$.

qRT-PCR. We used 50–200 mg of human renal tissue for total RNA extraction using the mirVana miRNA Isolation kit (Ambion, Life Technologies), following the manufacturer's protocol.

We extracted total RNA from mouse whole kidney by homogenization in TRIzol reagent (Invitrogen) and reverse-transcribed extracted RNA using the iScript kit (BioRad) according to the manufacturer's instructions. We analyzed expression of target genes by qRT-PCR on LightCycler 480 (Roche) using the qPCR Core kit for SYBR Assay (Eurogentec SA). We designed specific primers using Primer 3 (ref. 51) (primer sequences and PCR conditions available upon request). We determined amplification efficiency by dilution curves. We normalized *UMOD* expression in human samples to *NKCC2* (*SLC12A1*), to account for TAL segment content in each renal tissue sample, and in mouse samples to *Hprt1*. We calculated the relative mRNA expression of genes of interest following the $\Delta\Delta C_T$ method[52].

Histology. We performed routine staining (PAS, Trichrome and H&E) according to standard techniques. We stained heart sections with H&E for evaluation by light microscopy, capturing digital images with a Mirax Midi digital camera (Zeiss).

We used PAS-stained renal sections (three sections per mouse or patient) for the quantification of histological features. The sections were independently examined and scored by two observers unaware of the mouse or patient genotype. Sections were viewed using a Zeiss Axioscope 40FL microscope (Carl Zeiss) equipped with an AxioCam MRc5 digital video camera. Images were recorded using AxioVision software 4.3 (Carl Zeiss). We assessed mesangial expansion and capillary loop dilation semiquantitatively (0, absent; 1, 1–50%; 2, 51–100% of the tuft area), as we did for interstitial inflammation and fibrosis, presence of tubular casts and tubular dilation (0, absent; 1, 1–30%; 2, 31–60%; 3, 61–100% of the whole section area). We quantified the presence of segmental and global glomerulosclerosis as percentage of the total number of glomeruli.

In mouse renal sections, we scored vascular damage as present or absent and quantitatively determined tunica media width in at least six vessels (average value of five or six measurements per vessel) per organ ($n = 5$ per group).

Immunofluorescence and immunohistochemistry. Kidney sections (4–5 μm thick) were first deparaffinized by heating for 60 min at 56 °C and subsequently hydrated in the following solutions (5 min each): 2× xylene, 100% ethanol, 80% ethanol, 70% ethanol and cold tap water. Antigenic retrieval was obtained by incubation with heated citrate buffer (0.01 M, pH 6.0), twice for 2.5 min.

For immunofluorescence (IF), slides were blocked in either 10% bovine serum albumin or 10% donkey serum (1 h at room temperature) and incubated for 1 h at room temperature with primary antibody and for 1 h at room temperature

© 2013 Nature America, Inc. All rights reserved.

doi:10.1038/nm.3384

with appropriate AlexaFluor-labeled secondary antibody (Life Technologies, 1:500) All slides were viewed using a DM 5000B fluorescence upright microscope (Leica DFC480 camera, Leica DFC Twain Software, 40× 0.75 lens; Leica Microsystems) or an LSM510Meta Confocal microscope (Zeiss) equipped with a 40× 1.4 Plan-Apochromat oil-immersion objective (Zeiss). We used identical acquisition parameters for the same antibody in different kidney sections.

Immunohistochemistry (IHC) was performed following standard protocols. Briefly, after antigen retrieval, sections were incubated for 15 min in 3% H_2O_2 to quench endogenous peroxidase activity. Sections were then blocked with 10% normal goat serum and incubated for 1 h at room temperature with primary antibody, followed by incubation for 30 min at room temperature with the biotinylated secondary antibody (Vector Laboratories, 1:300) and peroxidase-labeled streptavidin (Invitrogen). Peroxidase activity was detected with 3,5-diaminobenzidine (Invitrogen). Sections were analyzed using a Zeiss Axioscope 40FL microscope equipped with an AxioCam MRc5 digital video camera (Carl Zeiss).

Immunoblotting. We homogenized mouse tissues from 6- to 24-week-old animals at 4 °C in lysis buffer (NaCl 150 mM, *N*-octylglucoside 60 mM, NaF 10 mM, Na_3VO_4 1 mM, glycerophosphate 1 mM, Protease-Inhibitor Cocktail 1:1,000 (Sigma-Aldrich) and Tris-HCl 20mM, pH 7.4). We obtained protein lysates from 16-month-old mice by solubilization of the tissue in lysis buffer, followed by sonication and centrifugation at 16,000*g* for 1 min at 4 °C, after which we used the supernatant. Alternatively, mouse tissues were homogenized in TRIzol (Invitrogen) and proteins were extracted after centrifugation at 11,000*g* for 15 min at 4 °C and collection of the organic phase that was then dialyzed against 0.1% SDS, precipitated with acetone and resuspended in PBS containing SDS 1%, NaF 10 mM, Na_3VO_4 1 mM, glycerophosphate 1 mM and Protease-Inhibitor Cocktail 1:1,000 (Sigma-Aldrich) (adapted from ref. 53). We analyzed the expression of Ncc and ENaC from kidney membrane preparations of 16-month-old mice as previously described[54]. Briefly, we homogenized kidneys in ice-cold lysis buffer (200 mM mannitol, 80 mM HEPES, 41 mM KOH, pH 7.5) with protease and phosphatase inhibitor cocktails (Complete ULTRA and PhosSTOP, Roche), obtained membrane preparations by ultracentrifugation (100,000*g*, 1 h, 4 °C) and solubilized in Laemmli buffer.

We obtained protein lysates from HEK cells 48 h after transfection by solubilizing the cells in lysis buffer (NaCl 0.4 M; EGTA 0.5 mM; $MgCl_2$ 1.5 mM, Hepes 10 mM, pH 7.9; glycerol 5% (v/v); Nonidet P-40 0.5% (v/v) and protease inhibitors (Complete, Roche Diagnostics)). We assessed total and phosphorylated Nkcc2 levels following immunoprecipitation with anti-Myc antibody (Clontech, 631206, 1:200). followed by affinity purification using protein G–agarose beads (Dynal). The purified immunocomplex was washed three times in PBS (Invitrogen).

Urinary proteins were precipitated with acetone, resuspended in PBS and subsequently loaded onto gels with normalization to urinary creatinine levels.

Protein lysates, immunoprecipitated proteins or urinary proteins were separated on 8–12% SDS-PAGE gel in nonreducing (total uromodulin) or in reducing (all other experiments) conditions and transferred onto nitrocellulose membrane (GE Healthcare). We performed western blotting (WB) following standard protocols. Quantification was performed using the gel analysis option of ImageJ software (http://rsbweb.nih.gov/ij/).

Antibodies. We used the following antibodies: sheep polyclonal (Abcam, ab9029-1, 1:200 for IF and for IHC) and goat polyclonal (MP Biomedicals, 55140, 1:1,000 for WB) antibodies against uromodulin, rat monoclonal antibody against HA (Roche, 11 867 423 001, 1:500 for IF and 1:1,000 for WB), rabbit polyclonal antibody against NKCC2 (Merck Millipore, AB3562P, 1:250 for IF and 1:1,000 for WB), rabbit polyclonal antibody against phospho-NKCC2 (phosphorylated Thr96 and Thr101)[55] (R5, 1:100 for IF and 1:750 for WB) (gift from B. Forbush), sheep antibody against SPAK (S150C, 1:1,000 for WB) and sheep polyclonal antibody against both phospho-SPAK (Thr243) and phospho-OSR1 (Thr185)[56] (S204C, 1:200 for IF and 1:2,000 for WB) (provided by D. Alessi), mouse monoclonal against OSR1 (OXSR1) (Abnova, H00009943-M09, 1:500 for WB), rabbit polyclonal against total NCC[54] (1:5,000 for WB), rabbit polyclonal against pT53NCC[54] (1:5,000 for WB), rabbit polyclonal against pT58NCC[54] (1:5,000 for WB), rabbit polyclonal against α-ENaC[54] (1:2,000 for WB), or rabbit polyclonal against γ-ENaC[57] (1:20,000 for WB), goat polyclonal antibody against renin (Santa Cruz Biotechnology, sc-27318, 1:500 for WB), rabbit polyclonal against ROMK (Chemicon, AB5196, 1:50 for IF), goat polyclonal against ROMK (Santa Cruz Biotechnology, sc-10692, 1:500 for WB), rabbit polyclonal antibody against aquaporin 2 (Sigma, A7310, 1:200 for IF), goat polyclonal against Lipocalin 2/NGAL (R & D Systems, AF1857, 1:500 for WB), rabbit polyclonal against KIM-1 (TIM-1) (Novus Biologicals, NBP1-76701, 1:500 for WB), rabbit polyclonal antibody against calnexin (Sigma, C4731, 1:20,000 for WB) and mouse monoclonal antibody against β-actin (Sigma, A2228, 1:20,000 for WB).

***In silico* analysis.** We analyzed the *UMOD* promoter sequence using Transcription Element Search Software (TESS) (http://www.cbil.upenn.edu/cgi-bin/tess/tess) or PATCH 1.0 (http://www.gene-regulation.com/pub/programs.html) and the associated Transfac database (Computational Biology and Informatics Laboratory, University of Pennsylvania). We aligned promoter sequences with Clustal Omega (http://www.ebi.ac.uk/Tools/msa/clustalo/) and displayed them with Jalview (http://www.jalview.org/)[58].

Statistical analyses. We performed comparisons between groups using a two-tailed unpaired Student's *t*-test, two-tailed nonparametric Mann-Whitney test or one-way ANOVA followed by Bonferroni's *post hoc* test (when three groups were compared). Only statistically significant pairwise comparisons are indicated in the figures. We used a mixed linear model to explore the association of *UMOD* rs4293393 with square-root–transformed daytime urinary uromodulin-to-creatinine ratio in order to better approximate a normal distribution of the residuals and to take familial correlations into account. We expressed continuous measures as mean ± s.d. and averages of measurements as mean ± s.e.m. We set the significance level to $P < 0.05$.

41. Manunta, P. *et al.* Physiological interaction between α-adducin and WNK1-NEDD4L pathways on sodium-related blood pressure regulation. *Hypertension* **52**, 366–372 (2008).
42. Pruijm, M. *et al.* Heritability, determinants and reference values of renal length: a family-based population study. *Eur. Radiol.* **23**, 2899–2905 (2013).
43. National Kidney Foundation. K/DOQI clinical practice guidelines for chronic kidney disease: evaluation, classification, and stratification. *Am. J. Kidney Dis.* **39**, S1–S266 (2002).
44. Youhanna, S. *et al.* Determination of uromodulin in human urine: influence of storage and processing. *Nephrol. Dial. Transplant.* doi:10.1093/ndt/gft345 (3 October 2013).
45. Dahan, K. *et al.* A cluster of mutations in the UMOD gene causes familial juvenile hyperuricemic nephropathy with abnormal expression of uromodulin. *J. Am. Soc. Nephrol.* **14**, 2883–2893 (2003).
46. Barr, D.B. *et al.* Urinary creatinine concentrations in the U.S. population: implications for urinary biologic monitoring measurements. *Environ. Health Perspect.* **113**, 192–200 (2005).
47. Bourgeois, S. *et al.* Differentiated thick ascending limb (TAL) cultured cells derived from SV40 transgenic mice express functional apical NHE2 isoform: effect of nitric oxide. *Pflugers Arch.* **446**, 672–683 (2003).
48. Terryn, S. A primary culture of mouse proximal tubular cells, established on collagen-coated membranes. *Am. J. Physiol. Renal Physiol.* **293**, F476–F485 (2007).
49. Glaudemans, B. *et al.* A primary culture system of mouse thick ascending limb cells with preserved function and uromodulin processing. *Pflugers Arch.* doi:10.1007/s00424-013-1321-1 (26 July 2013).
50. Zaarour, N., Demaretz, S., Defontaine, N., Mordasini, D. & Laghmani, K. A highly conserved motif at the COOH terminus dictates endoplasmic reticulum exit and cell surface expression of NKCC2. *J. Biol. Chem.* **284**, 21752–21764 (2009).
51. Rozen, S. & Skaletsky, H. Primer3 on the WWW for general users and for biologist programmers. *Methods Mol. Biol.* **132**, 365–386 (2000).
52. Pfaffl, M.W. A new mathematical model for relative quantification in real-time RT-PCR. *Nucleic Acids Res.* **29**, e45 (2001).
53. Hummon, A.B., Lim, S.R., Difilippantonio, M.J. & Ried, T. Isolation and solubilization of proteins after TRIzol extraction of RNA and DNA from patient material following prolonged storage. *Biotechniques* **42**, 467–470, 472 (2007).
54. Sorensen, M.V. *et al.* Rapid dephosphorylation of the renal sodium chloride cotransporter in response to oral potassium intake in mice. *Kidney Int.* **83**, 811–824 (2013).
55. Flemmer, A.W., Gimenez, I., Dowd, B.F.X., Darman, R.B. & Forbush, B. Activation of the Na-K-Cl cotransporter NKCC1 detected with a phospho-specific antibody. *J. Biol. Chem.* **277**, 37551–37558 (2002).
56. Rafiqi, F.H. *et al.* Role of the WNK-activated SPAK kinase in regulating blood pressure. *EMBO Mol. Med.* **2**, 63–75 (2010).
57. Wagner, C.A. *et al.* Mouse model of type II Bartter's syndrome. II. Altered expression of renal sodium- and water-transporting proteins. *Am. J. Physiol. Renal Physiol.* **294**, F1373–F1380 (2008).
58. Waterhouse, A.M., Procter, J.B., Martin, D.M., Clamp, M. & Barton, G.J. Jalview Version 2–a multiple sequence alignment editor and analysis workbench. *Bioinformatics* **25**, 1189–1191 (2009).

© 2013 Nature America, Inc. All rights reserved.